Regulation of morphine-induced synaptic alterations: Role of oxidative stress, ER stress, and autophagy

Yu Cai,[1] Lu Yang,[3] Guoku Hu,[1] Xufeng Chen,[4] Fang Niu,[1] Li Yuan,[1] Han Liu,[1] Huangui Xiong,[1] Jyothi Arikkath,[1,2] and Shilpa Buch[1]

[1]Department of Pharmacology and Experimental Neuroscience and [2]Developmental Neuroscience, Munroe-Meyer Institute, University of Nebraska Medical Center, Omaha, NE 68198
[3]School of Medicine, University of Electronic Science and Technology of China, Chengdu, Sichuan 610051, China
[4]Department of Emergence, The First Affiliated Hospital of Nanjing Medical University, Nanjing, Jiangsu 210029, China

Our findings suggest that morphine dysregulates synaptic balance in the hippocampus, a key center for learning and memory, via a novel signaling pathway involving reactive oxygen species (ROS), endoplasmic reticulum (ER) stress, and autophagy. We demonstrate in this study that exposure of morphine to hippocampal neurons leads to a reduction in excitatory synapse densities with a concomitant enhancement of inhibitory synapse densities via activation of the μ opioid receptor. Furthermore, these effects of morphine are mediated by up-regulation of intracellular ROS from NADPH oxidase, leading, in turn, to sequential induction of ER stress and autophagy. The detrimental effects of morphine on synaptic densities were shown to be reversed by platelet-derived growth factor (PDGF), a pleiotropic growth factor that has been implicated in neuroprotection. These results identify a novel cellular mechanism involved in morphine-mediated synaptic alterations with implications for therapeutic interventions by PDGF.

Introduction

Opioids such as morphine are the most potent and efficacious drugs currently available for pain management (Fields, 2011). Although these are widely used clinically, in addition to their beneficial analgesic effects, abuse of opioids such as morphine often results in deleterious side effects such as opioid tolerance, addiction, and detrimental effects on cognitive performance (Fields and Margolis, 2015). Emerging evidence suggests that neural circuits underlying addiction share some common pathways with those underlying learning and memory (Hyman et al., 2006). Morphine interferes with learning and memory processes in both healthy individuals and patients with cancer (Hill and Zacny, 2000; Kurita et al., 2011). Identifying molecular aberrations underlying morphine abuse that lead to cognitive changes and providing avenues for reversing these changes remains a pressing need in the field.

The hippocampus, an integrative center for regulating learning and memory and addiction (Koob and Volkow, 2010), is also one of the brain regions with significant expression for one of the major receptors for morphine, the μ opioid receptor (MOR; Le Merrer et al., 2009), suggesting that the effects of opioids on cognition could be mediated by signaling via MOR in hippocampus.

Alterations in synaptic density, structure, function, and plasticity have been identified as key components of the finely tuned machinery underlying cognition in hippocampus (Marder and Goaillard, 2006). Such mechanisms operate at both excitatory and inhibitory synapses (Nelson and Valakh, 2015).

Both in vitro and in vivo studies have demonstrated that morphine regulates excitatory spine density in hippocampus (Robinson et al., 2002; Zheng et al., 2010). However, our knowledge of the molecular mechanisms that underlie the ability of morphine to regulate spines and excitatory synapses remains far from complete. The effects of morphine on inhibitory synapses remain unclear. The balance of excitatory and inhibitory synapses is crucial for maintenance of normal functioning of neural circuits and higher-order brain functions including cognition (Froemke et al., 2007). There are limited avenues for therapeutic intervention to address cognitive deficits resulting from long-term use of morphine. Identifying molecular mechanisms underlying morphine-mediated synaptic alteration is thus of critical importance in our understanding of how neural circuitry responds to opioids and could provide insights into the

Correspondence to Jyothi Arikkath: jyothi.arikkath@unmc.edu; or Shilpa Buch: sbuch@unmc.edu

Abbreviations used: 3-MA, 3-methyladenine; 4-PBA, 4-phenylbutyrate; ANOVA, analysis of variance; ATF, activating transcription factor; BIP, binding Ig protein; DIV, days in vitro; GAD65, glutamic acid decarboxylase 65; H_2DCFDA, 2',7'-dichlorodihydrofluorescein diacetate; IRE1α, inositol-requiring protein 1α; mEPSC, miniature excitatory postsynaptic current; mIPSC, miniature inhibitory postsynaptic current; MOR, μ opioid receptor; PBN, phenyl-*N*-tert-butylnitrone; PERK, protein kinase R–like ER kinase; PSD95, postsynaptic density protein 95; ROS, reactive oxygen species; UPR, unfolded protein response; vGlut1, vesicular glutamate transporter 1.

The Rockefeller University Press $30.00
J. Cell Biol. Vol. 215 No. 2 245–258
https://doi.org/10.1083/jcb.201605065

development of therapeutic targets aimed at restoring normal cognitive function in morphine users.

We have identified a key signaling pathway that allows morphine signaling via MOR to regulate both excitatory and inhibitory synaptic density in hippocampus. Our data indicate that morphine-mediated activation of MOR results in the generation of reactive oxygen species (ROS), leading to downstream effects including activation of ER stress pathways followed by initiation of autophagy cascade. This eventually results in a decrease in excitatory synapse density accompanied by an increase in the density of inhibitory synapses, which likely contributes to the cognitive decline associated with morphine use. Promisingly, the detrimental effects of morphine on the density of both excitatory and inhibitory synapses can be ameliorated by PDGF-BB. Members of the PDGF family not only regulate neural development but also function as broad-acting neuroprotective agents (Cheng and Mattson, 1995; Tang et al., 2010). These studies thus provide a key mechanistic link between morphine use and cognitive decline and offer a potential avenue for preventing, or perhaps reversing, these cognitive deficits.

Results

Morphine alters the densities of excitatory and inhibitory synapses in the hippocampus

Morphine abuse is associated with cognitive changes that are likely linked to synaptic alterations. We used an in vivo model to examine if morphine administration altered the densities of excitatory and inhibitory synapses in the hippocampus, a key center for learning and memory. Groups of mice were exposed to either saline or morphine with intraperitoneal injection three times a day, starting at an initial dose of 10 mg/kg followed by ramping the dose by 5 mg/kg/d for six consecutive days (Pal and Das, 2013). At the end of treatment, mice were sacrificed, and the hippocampus was subjected to immunostaining and confocal microscopy. Morphine administration resulted in significant decrease of density of excitatory synapses with a significant enhancement of density of inhibitory synapses in the stratum lucidum and radiatum areas of the hippocampus, as indicated by densities of presynaptic (vesicular glutamate transporter 1 [vGlut1] and glutamic acid decarboxylase 65 [GAD65; Fig. 1, A and B; and Fig. S1 A]) and postsynaptic markers (postsynaptic density protein 95 [PSD95] and gephyrin; Fig. 1, C and D; and Fig. S1 B]) for excitatory and inhibitory synapses, respectively. To elucidate whether the synaptic alterations in response to morphine were region specific, we examined the protein levels of excitatory and inhibitory synaptic markers in the hippocampus, cortex, and striatum from control or morphine-treated mice (Fig. S2). Consistent with the data in Fig. 1, A–D, the levels of both excitatory and inhibitory synaptic markers were significantly altered in the hippocampus (Fig. S2, A and B). Interestingly, no alterations were observed in either the cortex or striatum (Fig. S2, C–F). To further examine if morphine-mediated synaptic changes in the hippocampus could be attributed to transcriptional alterations, we examined the levels of transcripts for excitatory and inhibitory synaptic markers in hippocampi from control and morphine treated mice (Fig. S3). In the hippocampus, we observed a significant decrease in the transcript levels of excitatory synaptic markers (Fig. S3 A). However, the transcript levels of inhibitory markers remained unchanged (Fig. S3 A). Consistent with the lack of synaptic alterations in the cortex and striatum, there were no changes in the levels of transcripts encoding excitatory or inhibitory synaptic markers in these regions (Fig. S3, B and C). Collectively, these in vivo results suggested that: (a) morphine-mediated synaptic alterations are likely region specific; and (b) morphine likely regulates the levels of excitatory synaptic proteins via transcription and inhibitory synapses translationally.

We next sought to examine if we could recapitulate morphine-mediated synaptic alterations in an in vitro–dissociated neuronal cell culture system (Beaudoin et al., 2012). There are two advantages to this approach. Because primary culture model is predominantly neuronal in nature, if we observed synaptic alterations with morphine, it would indicate that these effects are mediated by a direct effect on neurons, as opposed to a secondary consequence of activation of other cell types in hippocampus, including microglia and astrocytes (Horvath et al., 2010; Vacca et al., 2013). In addition, this is a well-established tractable model that would allow the exploration of underlying mechanisms.

We exposed GFP-expressing rat primary hippocampal neurons at 20 d in vitro (DIV) to morphine (10 µM) for 24 h followed by immunostaining for presynaptic and postsynaptic markers for both excitatory and inhibitory synapses. The neurons were subjected to confocal microscopy and synapse densities for both types of synapses were quantitated. Similar to our in vivo findings, morphine exposure resulted in a significant loss in the density of both dendritic spines and excitatory synapses (Fig. 1, E and G) and enhanced the density of inhibitory synapses (Fig. 1, F and G). Morphine exposure promoted a decrease in the density of excitatory synapses with an increase in the density of inhibitory synapses in vitro. Collectively, the in vivo and in vitro data indicate that morphine regulates density of excitatory and inhibitory synapses and that these effects are mediated by its direct action on neurons.

To confirm that these effects on synapses are specifically mediated by morphine-mediated activation of MOR, we pretreated neurons with opioid receptor antagonist naltrexone (10 µM) 1 h before morphine treatment before subjecting neurons to immunostaining with synaptic markers, confocal microscopy, and quantitation of synaptic densities. Pretreatment of neurons with naltrexone significantly abrogated morphine-mediated loss of dendritic spines and excitatory synapses while suppressing up-regulation of inhibitory synapses (Fig. 1, H and I). The effects of morphine on synaptic densities are thus mediated by its ability to bind and activate MOR.

The role of oxidative stress in morphine-mediated synaptic alterations

We sought to examine the components of the cellular signaling pathway that allow morphine to regulate synapses. Morphine has been shown to induce oxidative stress via generation of ROS in both macrophages as well as in vivo in the spinal cord (Bhat et al., 2004; Ibi et al., 2011). We next examined whether exposure of hippocampal neurons to morphine resulted in increased production of ROS and also sought to identify the intracellular source of ROS.

We took advantage of the 2',7'-dichlorodihydrofluorescein diacetate (H_2DCFDA) fluorescence assay (Gomes et al., 2005) to measure ROS levels in primary rat neurons exposed to morphine. Morphine promoted ROS production in a time-dependent manner with the peak response in ∼1 h after exposure (Fig. 2, A and B). Mitochondria and NADPH oxidases

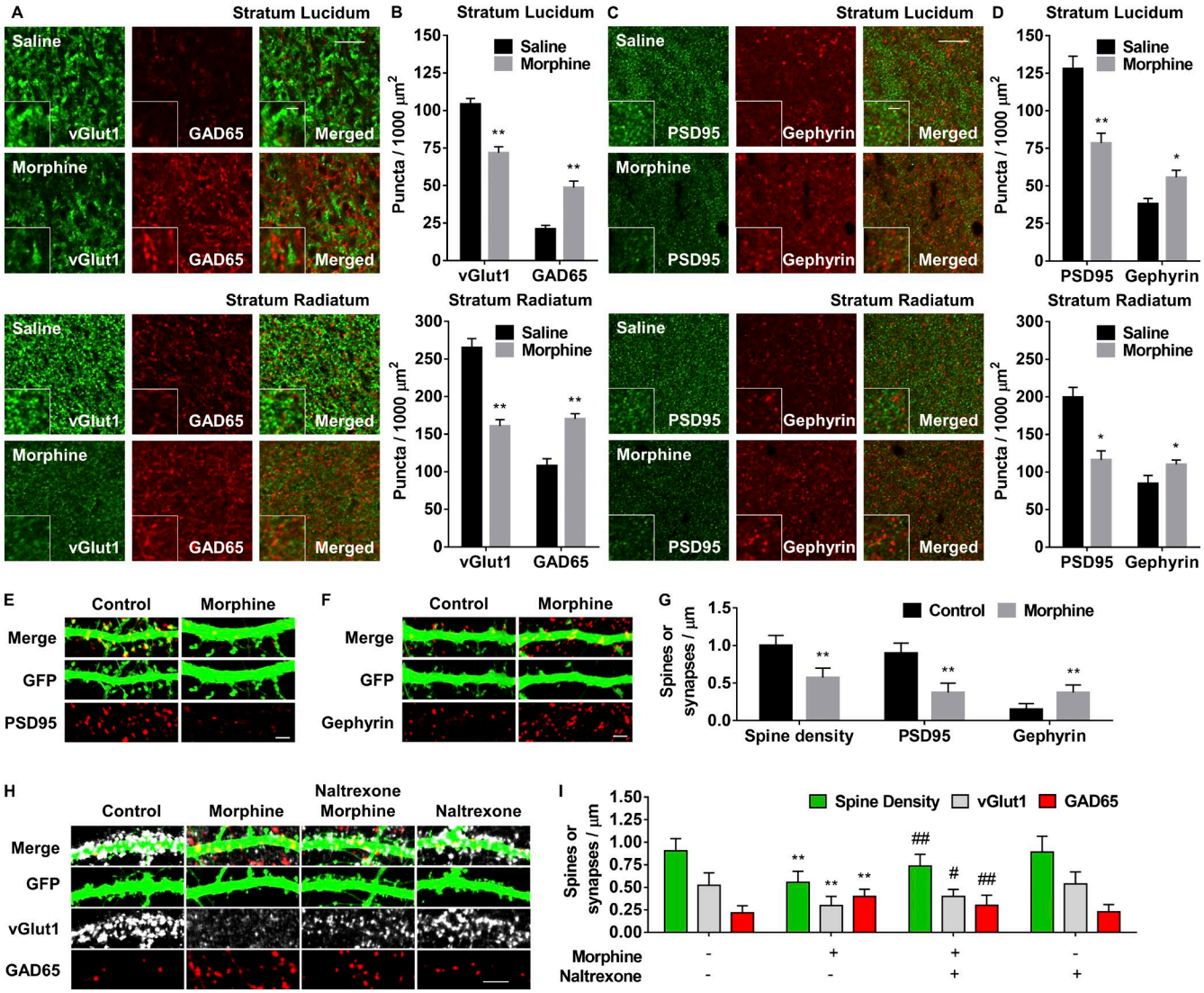

Figure 1. **Morphine alters the densities of excitatory and inhibitory synapses in the hippocampus.** Representative confocal images of the stratum lucidum and radiatum regions of mouse hippocampi were stained with presynaptic protein vGlut1 and GAD65 (A) and quantification of vGlut1 and GAD65 puncta (B). Bars: (top right) 10 µm; (inset) 2 µm. *n* = 6/group; Student's *t* test. Representative confocal images of the stratum lucidum and radiatum regions of mouse hippocampi stained with postsynaptic protein PSD95 and gephyrin (C) and quantification of PSD95 and gephyrin puncta (D). Bars: (top right) 10 µm; (inset) 2 µm. *n* = 6/group; Student's *t* test. (E) Representative confocal images of GFP-expressing primary rat hippocampal neurons (DIV 20) exposed to morphine (10 µM) for 24 h and immunostained for PSD95. Bar, 5 µm. (F) Representative confocal images of GFP-expressing primary rat hippocampal neurons treated with morphine and immunostained for gephyrin. Bar, 5 µm. (G) Quantification of spine density and excitatory and inhibitory synapses of E and F (Student's *t* test). Representative confocal images of GFP-expressing primary rat hippocampal neurons treated with naltrexone (10 µM) for 1 h followed by morphine for 24 h, stained with vGlut1 and GAD65 (H), and quantifications of spine density and excitatory and inhibitory synapses (I). Bar, 5 µm. One-way ANOVA with post hoc test. Each set of in vitro results was quantified upon four independent experiments. All data are presented as mean ± SD. *, P < 0.05; **, P < 0.01 versus control/saline group; #, P < 0.05; ##, P < 0.01 versus morphine group.

are the two major intracellular sources of ROS (Brennan et al., 2009; Shadel and Horvath, 2015). To determine the major contributing source of ROS after morphine exposure, neurons were pretreated with pharmacological inhibitors specific for either mitochondrial or NADPH oxidase ROS, exposed to morphine, and investigated for levels of ROS generated using the H_2DCF DA fluorescence assay. Pretreatment of cells with naltrexone (MOR antagonist), ROS scavenger phenyl-*N*-tert-butylnitrone (PBN), or inhibitor of NADPH oxidase apocynin significantly suppressed morphine-mediated induction of ROS generation (Fig. 2 C). Mitochondria-targeted antioxidant MitoTEMPO, however, failed to inhibit morphine-mediated induction of oxidative stress (Fig. 2 C). These results are thus consistent with a role for NADPH oxidase, but not that of mitochondria, in generating ROS in hippocampal neurons exposed to morphine.

To examine the relevance of morphine and NADPH oxidase-mediated ROS in regulating synapses, we performed experiments similar to that described for Fig. 1 F in neurons pretreated with NADPH oxidase inhibitor apocynin (10 µM). Pretreatment of cells with apocynin resulted in inhibition of morphine-mediated synaptic alterations, including down-regulation of both spine density and excitatory synapses with a concomitant up-regulation of inhibitory synapses (Fig. 2, D and E). These data are consistent with a model in which morphine-mediated ROS generation, via MOR, influences densities of excitatory and inhibitory synapses in hippocampal neurons.

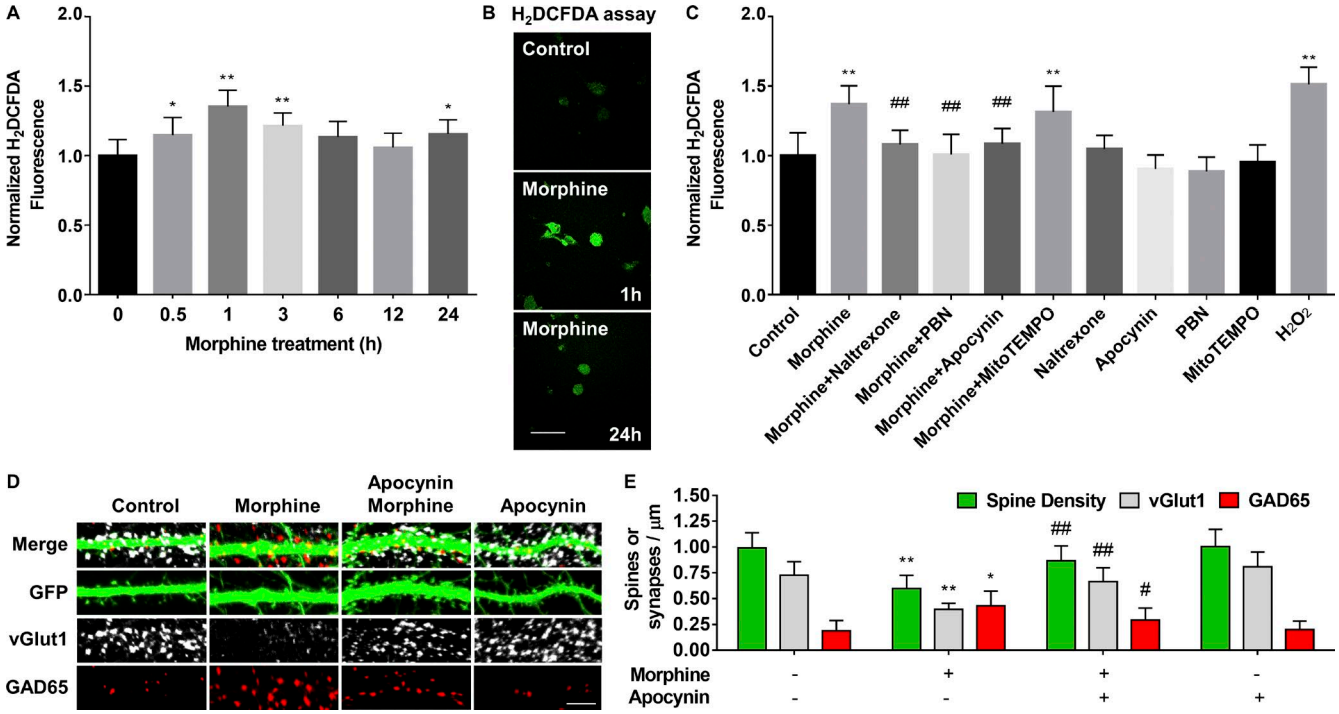

Figure 2. **The role of oxidative stress in morphine-mediated synaptic alterations.** (A) Time course of ROS generation in primary hippocampal neurons exposed to morphine by H_2DCFDA assay. (B) Representative H_2DCFDA assay images of neurons at 1 and 24 h after morphine exposure. Bar, 40 µm. (C) Neurons were pretreated with naltrexone, PBN (500 µM), apocynin (10 µM), or MitoTEMPO (100 µM) for 30 min followed by 1-h morphine treatment and assessed for ROS generation by H_2DCFDA assay. Representative confocal images of GFP-expressing primary rat hippocampal neurons treated with apocynin for 1 h followed by morphine for 24 h stained with vGlut1 and GAD65 antibodies (D) and quantifications of spine density and excitatory and inhibitory synapses (E). Bar, 5 µm. Each set of in vitro results was quantified upon four independent experiments. All data are presented as mean ± SD. *, $P < 0.05$; **, $P < 0.01$ versus control group; #, $P < 0.05$; ##, $P < 0.01$ versus morphine group using one-way ANOVA with post hoc test.

The role of ER stress in morphine-mediated synaptic alterations

We examined downstream mechanisms that link morphine-induced ROS generation to synaptic alterations. To this end, we focused on the ER stress pathway. The cellular redox status altered by ROS generation has been reported to affect ER protein folding, resulting in ER stress (Guo et al., 2015; Wang et al., 2015). In response to ER stress, there is an initiation of the unfolded protein response (UPR) that is induced as an adaptive mechanism, involving up-regulation of the three cascading sensors—protein kinase R–like ER kinase (PERK), inositol-requiring protein 1α (IRE1α), and activating transcription factor (ATF) 6—and the ER chaperone binding Ig protein (BIP; Cai et al., 2016a). Although ER stress triggered by oxidative stress has been suggested to play a crucial role in neurodegenerative diseases (Uehara et al., 2006), its effects in synaptic structure and function remain unclear.

To examine whether morphine exposure could induce ER stress, we investigated expression of several critical UPR mediators—BIP, phosphorylated PERK (pPERK), IRE1α, and ATF6—in hippocampus of mice exposed to morphine. Hippocampal lysates from mice with morphine injection were assessed for expression of UPR mediators by Western blots. There was a significant increase of the major UPR mediators in hippocampal lysates of morphine-injected mice compared with the saline-injected controls (Fig. 3, A and B). In addition, we found a time-dependent increase of BIP in primary hippocampal neurons exposed to morphine, indicating that morphine also triggered ER stress in vitro, consistent with our in vivo findings (Fig. 3, C and D). To confirm that these alterations are a direct consequence of the activation of MOR by morphine, we pretreated primary neurons in culture with MOR antagonist naltrexone before morphine exposure and examined expression of ER stress markers by Western blots. Pretreatment of neurons with naltrexone inhibited morphine-mediated increase of ER stress markers (Fig. 3, E and F). These studies thus indicated that morphine-mediated activation of MOR promotes ER stress and initiates the UPR response, both in vivo and in vitro.

Because morphine mediates ER stress in hippocampal neurons both in vitro and in vivo, we sought to assess the role of ER stress in morphine-mediated synaptic alterations. Pharmacological blocking of ER stress by 4-phenylbutyrate (4-PBA; a chaperone-like ER stress inhibitor) in primary rat hippocampal neurons resulted in attenuation of morphine-mediated induction of synaptic alterations (Fig. 3, G and H). We next explored the link between morphine-mediated induction of ER stress and oxidative stress. Morphine-mediated increase of ER stress regulators was ameliorated in hippocampal neurons pretreated with oxidative stress inhibitors PBN or apocynin (Fig. 3, I and J). In contrast, in neurons pretreated with the ER stress inhibitor 4-PBA, there was no change in morphine-mediated induction of ROS (Fig. 3 K). These results are consistent with a model in which morphine-mediated oxidative stress functions upstream of ER stress to regulate synaptic densities in hippocampal neurons.

The role of autophagy in morphine-mediated synaptic alterations

We have previously demonstrated that cocaine mediated induction of both ER stress as well as downstream autophagy to play

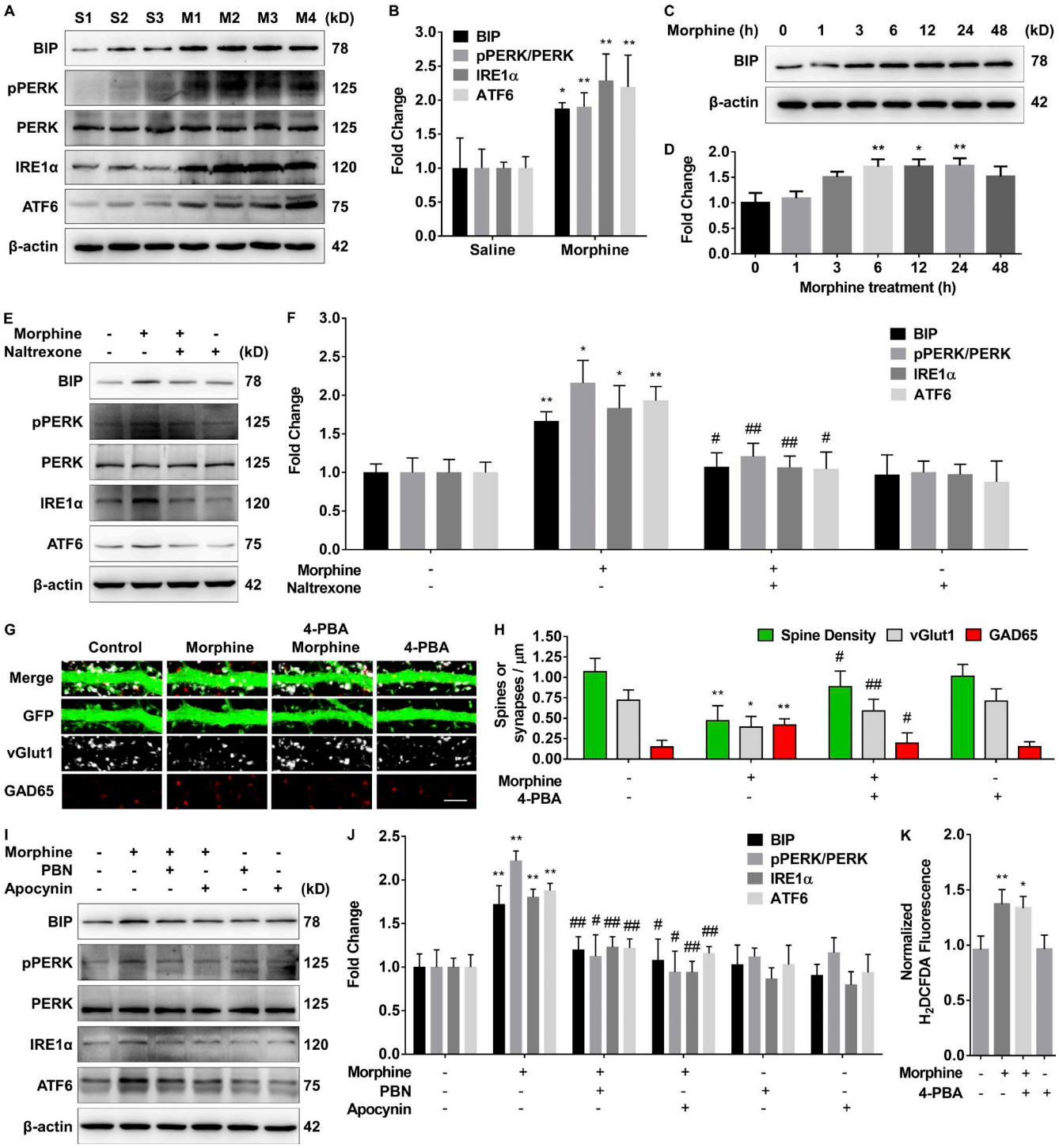

Figure 3. **The role of ER stress in morphine-mediated synaptic alterations.** Representative Western blot (A) and quantification of ER stress mediators (BIP, pPERK, IRE1α, and ATF6; B) in the hippocampal lysates from mouse injected with saline or morphine (n = 3 to 4/group; *, $P < 0.05$; **, $P < 0.01$ versus saline group using Student's t test). Representative time course Western blot (C) and quantification of BIP in primary neurons exposed to morphine (D). Representative Western blot (E) and quantification of BIP, pPERK, IRE1α, and ATF6 (F) in the cell lysates from neurons pretreated with naltrexone for 1 h followed by 24-h morphine treatment. Representative confocal images of GFP-expressing primary rat hippocampal neurons treated with 4-PBA (1 mM) for 1 h followed by morphine for 24 h and stained with vGlut1 and GAD65 (G) and quantifications of spine density and excitatory and inhibitory synapses (H). Bar, 5 μm. Representative Western blot (I) and quantification of BIP, pPERK, IRE1α, and ATF6 (J) in the cell lysates from neurons pretreated with PBN or apocynin for 1 h followed by 24-h morphine treatment. (K) H_2DCFDA assay of neurons pretreated with 4-PBA for 30 min followed by 1-h morphine treatment. Quantification of Western blot results were all normalized to β-actin, except that pPERK was normalized to PERK. Each set of in vitro results was quantified upon four independent experiments. All data are presented as mean ± SD. *, $P < 0.05$; **, $P < 0.01$ versus control group; #, $P < 0.05$; ##, $P < 0.01$ versus morphine using one-way ANOVA with post hoc test (except B).

a key role in microglial activation (Guo et al., 2015). Autophagy is an intracellular catabolic process that delivers intracellular organelles or misfolded proteins for lysosomal degradation (Cai et al., 2016a). Previous studies have demonstrated that morphine exposure leads to enhanced autophagic activity in both human neuroblastoma cell line as well as in the rat hippocampus (Zhao et al., 2010). Interestingly, neuronal autophagy has also been reported to play a key role in synaptic pruning (Tang et al., 2014).

Next, we examined whether morphine-mediated synaptic alterations involved up-regulation of autophagy. Western blots of hippocampal lysates from mice administrated morphine demonstrated that morphine exposure also resulted in induction of autophagy mediators, including Beclin1, ATG5, and LC3-II, with a concomitant down-regulation of the autophagy substrate protein p62 (Fig. 4, A and B). Consistent with our in vivo findings, exposure of primary hippocampal neurons to morphine resulted in increased expression of LC3-II in a time-dependent manner (Fig. 4, C and D). We examined the number of autophagosomes in primary neurons transfected with GFP-LC3 plasmids treated with morphine. As shown in Fig. 4, G and H, morphine exposure significantly increased number of GFP-LC3 puncta. Morphine exposure also up-regulated expression of Beclin1, ATG5, and LC3-II with a decrease in p62 levels in primary hippocampal neurons as examined by Western blots. This effect of morphine was reversed in cells pretreated with MOR antagonist naltrexone (Fig. 4, E and F).

To determine whether morphine mediated enhanced generation of autophagosomes, morphine-exposed primary rat neurons were treated with bafilomycin, an autophagy inhibitor (at a saturating concentration of 100 nM), to prevent fusion of autophagosomes with lysosomes (Shehata et al., 2012) and assessed for LC3-II expression. There was a significant increase in LC3-II levels (Fig. 4, I and J) in neurons exposed to both morphine and bafilomycin compared with bafilomycin alone, indicating that morphine induced autophagy via a stimulating autophagosome formation. To explore the role of autophagy in morphine-mediated synaptic alterations, GFP-expressing neurons were pretreated with an autophagy inhibitor, wortmannin, that suppresses formation of autophagosomes before morphine exposure. Pharmacological blocking of autophagy ameliorated morphine-mediated loss of spine density and excitatory synapses with an increase in inhibitory synapses (Fig. 4, K and L). To confirm that these results were specific for the autophagy pathway, we transfected neurons with PGK-GFP-shATG7 to specifically knock down ATG7, one of the key mediators for autophagic activity (Rodríguez-Muela et al., 2013; Fig. S4). Primary hippocampal neurons were transfected with either scramble shRNA or shRNA to ATG7, followed by morphine exposure and assessed for densities of both excitatory and inhibitory synapses. Consistent with the data using chemical inhibitors of autophagy, knocking down ATG7 in neurons alleviated the synaptic phenotype observed under the influence of morphine (Fig. 4, M and N). Collectively, these results indicate that autophagy is a critical regulator of morphine-mediated synaptic alterations.

Morphine-mediated autophagy in hippocampal neurons: The role of oxidative and ER stress

Having determined the involvement of oxidative stress, ER stress, and autophagy in morphine-mediated synaptic alterations, we next sought to examine the link between morphine-mediated oxidative and ER stress and autophagy. For this, primary hippocampal neurons were pretreated with various pharmacological inhibitors specific for oxidative or ER stress followed by exposure of cells to morphine and assessment of autophagic markers by Western blotting. As shown in Fig. 5, A and B, in the presence of oxidative stress inhibitors PBN or apocynin, morphine failed to up-regulate expression of major autophagy mediators such as Beclin1, ATG5, and LC3-II and also failed to down-regulate expression of autophagy substrate p62. Interestingly, autophagy inhibitor 3-methyladenine (3-MA) failed to have any effect on morphine-mediated ROS production (Fig. 5 C). Similarly, in presence of ER stress inhibitors such as 4-PBA or salubrinal, morphine failed to regulate autophagy mediators (Fig. 5, D and E). Reciprocally however, pretreatment of cells with autophagy inhibitors such as wortmannin or 3-MA had no effect on morphine-mediated up-regulation of ER stress proteins (Fig. 5, F and G). Collectively, these findings indicate that both oxidative and ER stress are upstream of morphine-mediated autophagy.

Protective role of PDGF-BB in morphine-mediated synaptic alterations

Our previous studies have demonstrated a neuroprotective role of PDGF-BB in both primary cortical neurons and human neuroblastoma cell line against HIV proteins gp120 and Tat (Peng et al., 2008; Zhu et al., 2009). We have also previously demonstrated that exposure of hippocampal neurons to PDGF-BB leads to induction of the gene Arc/Arg3.1 (Peng et al., 2010), a synaptic plasticity gene that plays a critical role in learning and memory formation (Cao et al., 2015; Gouty-Colomer et al., 2016). Moreover, PDGF-BB is also known to protect hippocampal neurons against apoptosis induced by glucose deprivation or an oxidative insult (Cheng and Mattson, 1995). We thus rationalized that exposure of morphine-treated neurons to PDGF-BB could also lead to protection against morphine-mediated impairment of synaptic alterations via its effects on ROS and downstream ER stress and autophagy. To verify this, hippocampal primary neurons (DIV 20) were treated with PDGF-BB (20 ng/ml) for 24 h after exposure to morphine. After treatment, neurons were fixed, immunostained for synaptic markers, and subjected to confocal microscopy to assess synaptic densities. In neurons treated with PDGF-BB, morphine exposure did not alter synaptic densities, unlike neurons exposed to morphine, suggesting that PDGF-BB treatment resulted in significant protection against morphine-mediated alterations in synaptic densities (Fig. 6, A and B). To examine the functional alterations induced by morphine treatment followed by rescue with PDGF-BB, we recorded frequencies of miniature excitatory postsynaptic currents (mEPSCs) and miniature inhibitory postsynaptic currents (mIPSCs) in primary neurons (DIV 19–21) treated with saline, morphine, PDGF-BB, or morphine plus PDGF-BB (Fig. 6, C–F). Consistent with the in vivo and in vitro data, we observed a decrease in the frequency of mEPSCs with a concomitant increase in frequencies of mIPSCs in neurons treated with morphine. Thus, morphine-induced alterations in synaptic densities were reflected as functional alterations at synapses. In addition, consistent with the data shown in Fig. 6 (A and B), PDGF-BB treatment rescued the effects of morphine treatment, as was evident by the frequencies of mIPSCs and mEPSCs (Fig. 6, C–F).

PDGF-BB exposure also resulted in amelioration of morphine-mediated ROS production (Fig. 6 G) as examined by H_2DCFDA fluorescence assay. Furthermore, Western blots also

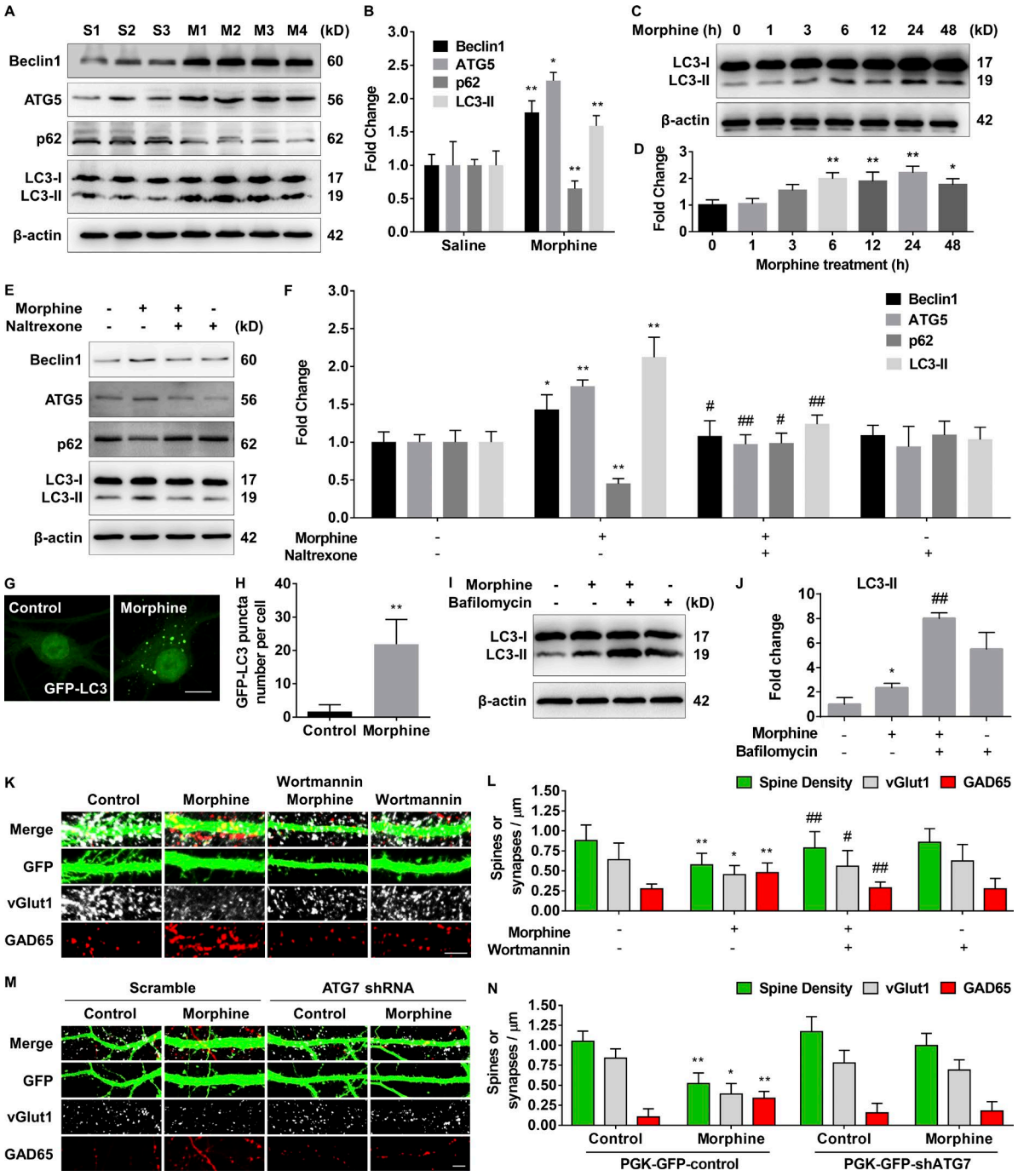

Figure 4. **The role of autophagy in morphine-mediated synaptic alterations.** Representative Western blot (A) and quantification of autophagy mediators (Beclin1, ATG5, p62, and LC3-II; B) in the hippocampal lysates from mouse injected with saline or morphine (n = 3 to 4/group). *, $P < 0.05$; **, $P < 0.01$ versus saline group using Student's t test. Representative time course Western blot (C) and quantification of LC3-II (D) in primary neurons exposed to morphine. Representative Western blot (E) and quantification of Beclin1, ATG5, p62, and LC3-II (F) in the cell lysates from neurons pretreated with naltrexone for 1 h followed by 24-h morphine treatment. Representative confocal images (G) and quantification of GFP-LC3 puncta (H) of primary hippocampal neurons expressing GFP-LC3 exposed to morphine for 24 h. Bar, 10 μm. **, $P < 0.01$ versus saline group using Student's t test. Representative Western blot (I) and quantification of LC3-II (J) in the cell lysates of neurons treated with bafilomycin for 4 h after 24-h exposure to morphine. Representative confocal images of GFP-expressing primary rat hippocampal neurons treated with wortmannin (500 μM) for 1 h followed by morphine exposure for 24 h and stained with vGlut1 and GAD65 (K) and quantifications of spine density and excitatory and inhibitory synapses (L). Bar, 5 μm. Representative confocal images of neurons expressing PGK-GFP-scramble or PGK-GFP-shATG7 vector in the presence or absence of morphine for 24 h and stained with vGlut1 and GAD65 (M) and quantifications of spine density and excitatory and inhibitory synapses (N). Bar, 5 μm. Quantification of Western blot results were all normalized to β-actin. Each set of in vitro results was quantified upon four independent experiments. All data are presented as mean ± SD. *, $P < 0.05$; **, $P < 0.01$ versus control group; #, $P < 0.05$; ##, $P < 0.01$ versus morphine group using one-way ANOVA with post hoc test (except B and H).

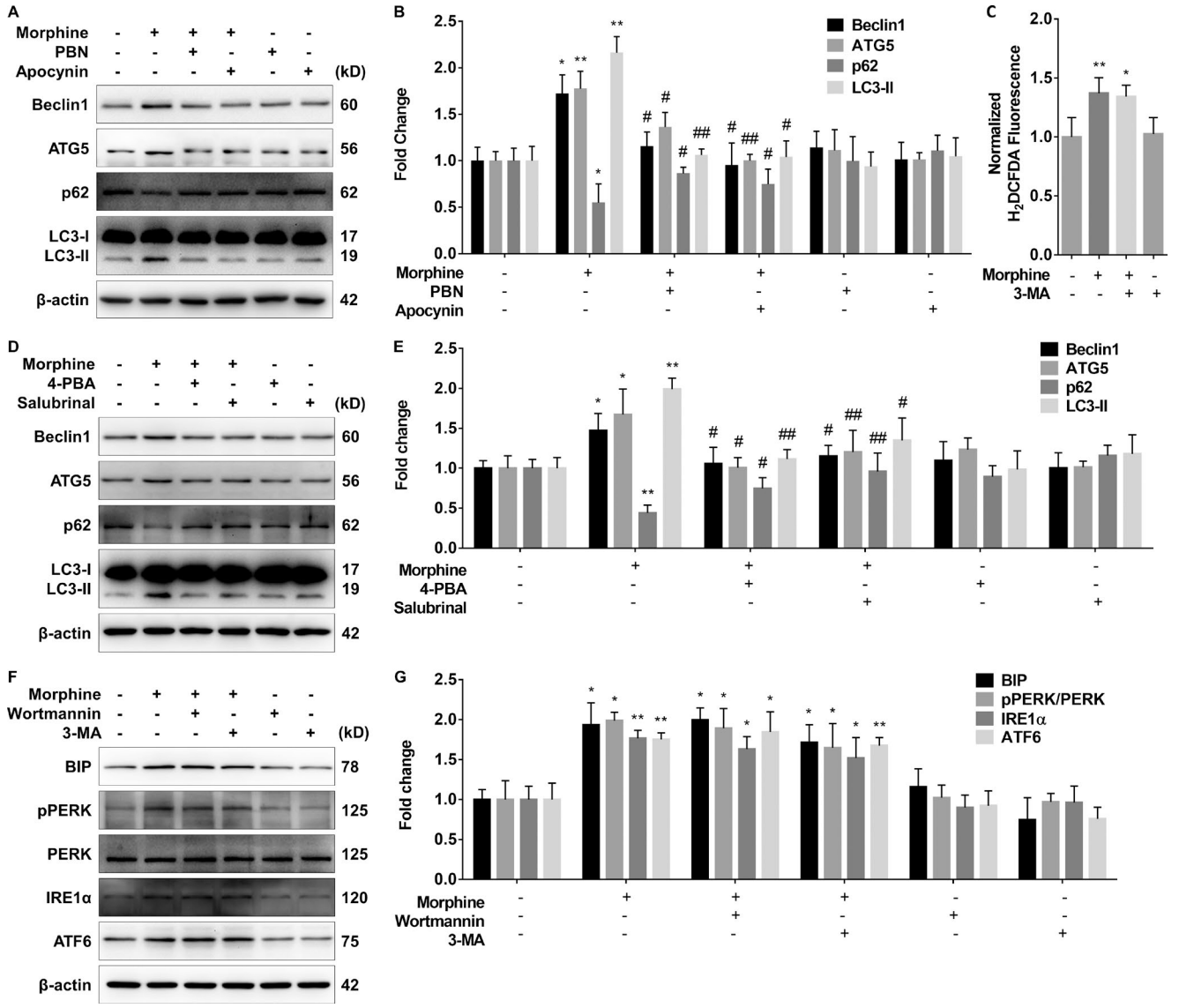

Figure 5. **Morphine-mediated autophagy in hippocampal neurons: Role of oxidative and ER stress.** Representative Western blot (A) and quantification of autophagy mediators (Beclin1, ATG5, p62, and LC3-II; B) in the cell lysates of neurons pretreated with PBN or apocynin for 1 h followed by 24-h morphine treatment. (C) H_2DCFDA assay of neurons pretreated with 3-MA (50 µM) for 30 min followed by morphine exposure. Representative Western blot (D) and quantification of Beclin1, ATG5, p62, and LC3-II (E) in the cell lysates of neurons pretreated with 4-PBA or salubrinal (100 µM) for 1 h followed by 24-h morphine exposure. Representative Western blot (F) and quantification of BIP, pPERK, IRE1α, and ATF6 (G) in the cell lysates of neurons pretreated with wortmannin or 3-MA for 1 h followed by 24-h morphine exposure. Quantification of Western blot results were all normalized to β-actin, except that pPERK was normalized to PERK. Each set of our results was quantified upon four independent experiments. All data are presented as mean ± SD. *, $P < 0.05$; **, $P < 0.01$ versus control/saline group; #, $P < 0.05$; ##, $P < 0.01$ versus morphine group using one-way ANOVA with post hoc test.

indicated that PDGF-BB treatment prevented the activation of ER stress (Fig. 6, H and I) and autophagy (Fig. 6, J and K) pathways that lie downstream of morphine-mediated oxidative stress. Collectively, these results indicate that treatment of neurons with PDGF-BB is beneficial in ameliorating morphine-mediated synaptic alterations by inhibiting the generation of the upstream ROS that triggers activation of ER stress and autophagy pathways.

Discussion

Morphine and related opioids are widely used clinically resulting in beneficial analgesic effects. However, prolonged use of morphine can also promote deleterious effects including opioid tolerance, addiction, and cognitive decline (Fields and Margolis, 2015). Morphine use interferes with learning and memory processes (Hill and Zacny, 2000; Hearing et al., 2016). Learning and memory are intimately linked to the structure, function, and plasticity of synapses (Smolen et al., 2016). Although the majority of studies have demonstrated significant reduction in dendritic spine density in the nucleus accumbens, hippocampus, and neocortex of adult rats with morphine (Robinson et al., 2002), our understanding of the molecular basis of how morphine leads to the cellular alterations that contribute to cognitive decline is scant (Robinson et al., 2002; Marder and Goaillard, 2006; Mazei-Robison et al., 2011), thus limiting options to provide effective therapeutic interventions to ameliorate cognitive decline associated with long-term morphine use. Our studies identify a novel linear pathway linking morphine-mediated

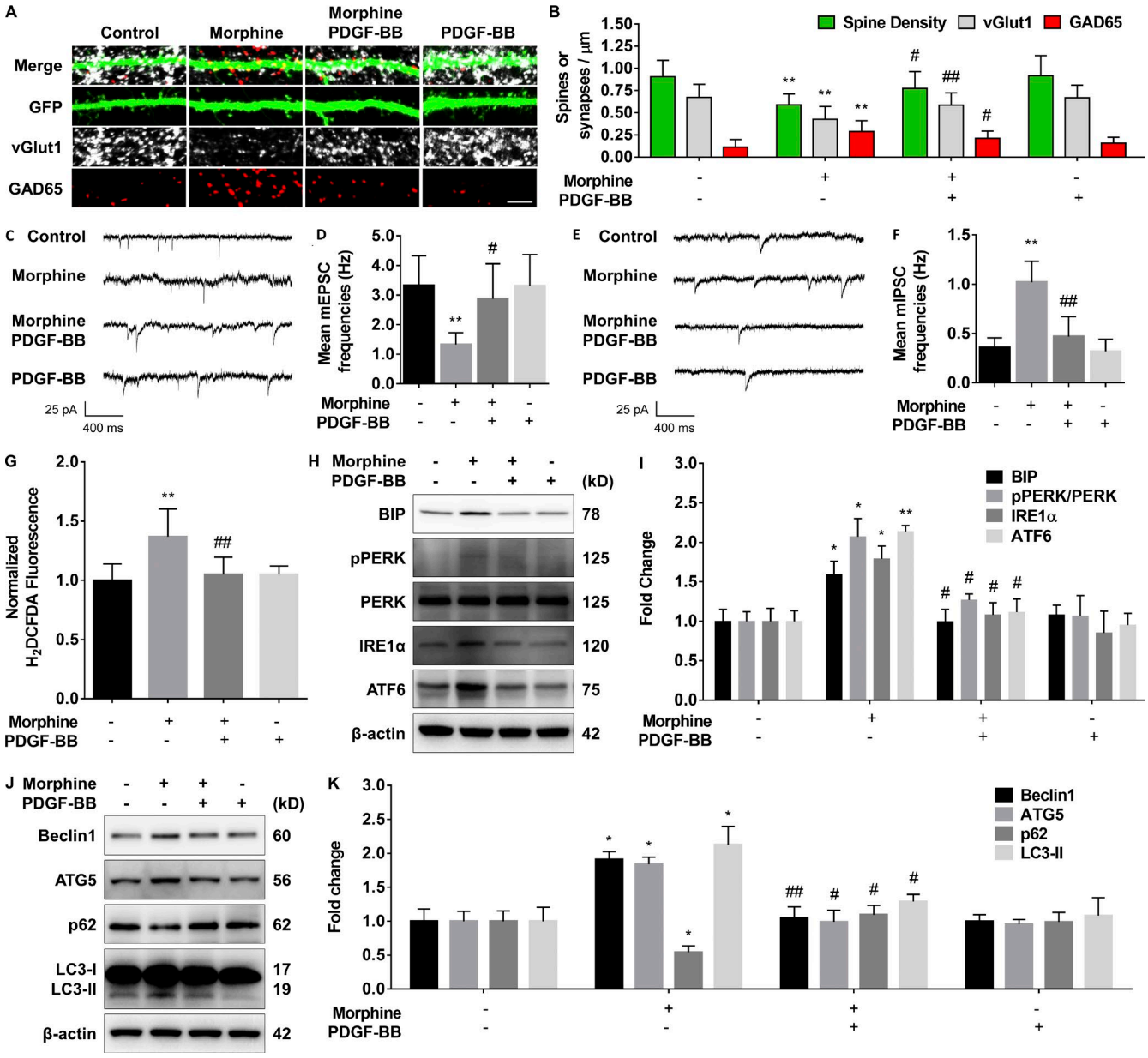

Figure 6. **Protective role of PDGF-BB in morphine-mediated synaptic alterations.** Representative confocal images of GFP-expressing primary rat hippocampal neurons exposed to morphine followed by treatment with PDGF-BB (20 ng/ml) and stained with vGlut1 and GAD65 (A) and quantifications of spine density and excitatory and inhibitory synapses (B). Bar, 5 μm. Representative traces of whole-cell voltage-clamp recording showing mEPSC (C), mIPSC (E), mean mEPSC frequencies (D), and mean frequencies of mIPSCs (Hz; F) in primary rat neurons (DIV 19–21) treated with combinations of saline, morphine, and PDGF-BB as indicated. (G) ROS generation in neurons exposed to morphine and treated with PDGF-BB. Representative Western blot (H) and quantification of BIP, pPERK, IRE1α, and ATF6 (I) in the cell lysates of neurons exposed to morphine followed by treatment with PDGF-BB (20 ng/ml) for an additional 24 h. Representative Western blot (J) and quantification of Beclin1, ATG5, p62, and LC3-II (K) in the cell lysates of neurons exposed to morphine for 24 h followed by PDGF-BB (20 ng/ml) for additional 24 h. Quantification of Western blot results were all normalized to β-actin except that pPERK was normalized to PERK. Each set of our results was quantified upon four independent experiments. All data are presented as mean ± SD. *, $P < 0.05$; **, $P < 0.01$ versus control/saline group; #, $P < 0.05$; ##, $P < 0.01$ versus morphine group using one-way ANOVA with post hoc test.

activation of MOR in neurons to alterations in excitatory and inhibitory synapse densities in hippocampus, thus providing a novel mechanism for morphine-induced cognitive changes. More importantly, we provide key evidence that morphine-induced synaptic alterations can be prevented by treating neurons with PDGF-BB, a pleiotropic neuroprotective agent (Peng et al., 2008; Zhu et al., 2009; Keller et al., 2013; Yang et al., 2015). Interestingly, these synaptic alterations were mainly observed in the hippocampus, but not in the striatum or cortex, suggesting that the effects of morphine were region specific and that the synaptic alterations in the hippocampus could likely contribute to the cognitive changes observed after morphine exposure. These studies thus underscore a molecular mechanism for cognitive changes associated with morphine use and a strategy for ameliorating these deficits.

Our data provide evidence that morphine-mediated activation of the MOR in hippocampal neurons results in sequential generation of ROS, ER stress, and autophagy, leading to a decrease in density of excitatory and increase in density of inhibitory synapses (Fig. 7). Morphine-mediated synaptic

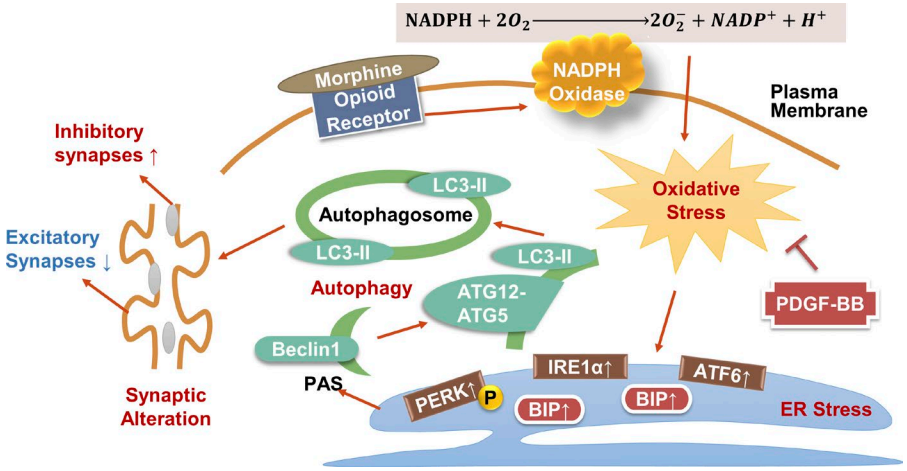

Figure 7. **Schematic of morphine-mediated synaptic alterations.** Synaptic alterations induced by morphine involve a novel mechanism that requires sequential activation of MOR, oxidative stress, ER stress, and autophagy. PDGF-BB ameliorates morphine-mediated synaptic alterations at the level of ROS generation and its downstream signaling.

alterations in synaptic density and function could be reversed by PDGF-BB. The protective effects of PDGF-BB are mediated at the level upstream of ROS generation and by preventing activation of downstream ER stress and autophagy pathways.

Interestingly, similar cellular signaling pathways also exist in other cell types including microglia and cardiomyoblasts, where they are harnessed for other functional roles including inflammatory and apoptotic responses (Younce and Kolattukudy, 2010; Guo et al., 2015). Our data on the significance of these pathways for neuronal function, particularly in regulating synapses, are novel.

A role for ROS in morphine-mediated synaptic regulation

The highly metabolic nature of the brain results in the robust production of ROS in neurons, for which levels are maintained through a network of antioxidants. At physiologically relevant concentrations, ROS has been demonstrated to participate in cellular mechanisms that underlie synaptic plasticity and hence cognitive functions (Massaad and Klann, 2011). Excessive levels of ROS are also associated with decreases in cognitive performance. The ability of morphine to elicit alterations in ROS levels is consistent with data from other cells such as murine macrophages and microglia (Bhat et al., 2004; Cai et al., 2016b).

Although several sources for generation of ROS exist in neurons (Brennan et al., 2009; Shadel and Horvath, 2015), our data indicate that morphine activation of MOR specifically harnesses the NADPH oxidase pathway for ROS generation, which, in turn, activates a specific downstream signaling pathway to promote synaptic changes. Targeting NADPH oxidase–mediated ROS generation could thus be envisioned as a viable target to ameliorate synaptic alterations induced by morphine.

ER stress contributes to morphine-mediated synaptic alterations

The ER is a subcellular compartment that governs protein quality control in the secretory pathway to prevent protein aggregation and misfolding (Cai et al., 2016a). Activation of ER stress promotes the UPR to re-establish homoeostasis. Although the role of these pathways in relation to neurodegenerative disorders has been explored (Hetz and Mollereau, 2014), it remains unclear how ER stress, independent of cell death, contributes to other neuronal processes including synaptic alterations. Although ER stress (Huang et al., 2015) and components of the UPR response have been linked to deficits in learning and memory (Martínez et al., 2016), the underlying mechanisms remain incompletely understood.

Our study provides the first direct link between morphine and ER stress and indicates that morphine activation via MOR and ROS-mediated signaling promotes up-regulation of both ER chaperone protein BIP and the three major arms of ER stress (pPERK, IRE1α, and ATF6) that eventually regulate both excitatory and inhibitory synapses. Interestingly, pretreatment of neurons with a chaperone-like ER stress inhibitor 4-PBA significantly abrogated morphine-mediated synaptic loss, suggesting another viable target for therapeutic intervention in morphine-mediated cognitive decline.

The role of autophagy in morphine-mediated regulation of excitatory and inhibitory synapses

Autophagy is an intracellular process that delivers cellular organelles and misfolded proteins from the autophagosomes to the lysosomes for degradation (Zhang and Baehrecke, 2015). Substances of abuse such as cocaine and morphine have been shown to induce autophagy in the human neuroblastoma cell line SH-SY5Y and rat hippocampus (Zhao et al., 2010) and microglia (Guo et al., 2015).

Our understanding of the link between autophagy and synaptic structure and function in absence of neurodegeneration (Menzies et al., 2015; Martini-Stoica et al., 2016) has been limited. Recent studies have implicated a role for autophagy in spine pruning associated with autism (Tang et al., 2014) via an mammalian target of rapamycin complex 1–dependent pathway. However, there are no reported studies that link autophagy to the morphogenesis of inhibitory synapses.

Our studies indicate that morphine-mediated induction of autophagy regulates both excitatory and inhibitory synapses. Moreover, we demonstrate that morphine initiates the autophagy cascade via a sequential activation of ROS and ER stress pathways and results in enhanced autophagosome formation. In addition to the implications of these studies for morphine-mediated synaptic changes, this is the first study to implicate a role for autophagy in the regulation of inhibitory synapses. How induction of autophagy leads to alterations in synaptic densities, particularly inhibitory synapses, remains to be identified. During the development of hippocampus, excessive synapses are generated before active pruning to generate a fairly stable synaptic pool (Tang et al., 2014). It is conceivable that autophagic mechanisms operate either at

the level of synapse generation or synaptic pruning to control synaptic densities.

Morphine-mediated synaptic alterations and cognition

Neural circuits are regulated by activity-dependent feedback that tightly controls neural excitability. Deficits or imbalances in excitation and inhibition can have serious consequences that contribute to pathological conditions. Such perturbations are frequently observed in neurodevelopmental disorders associated with cognitive disabilities (Sandi and Haller, 2015). Thus, morphine-mediated alterations in the balance of excitatory and inhibitory synapses are likely to contribute to deficits in the neural circuits underlying cognition.

PDGF-BB–mediated protection against morphine-induced synaptic alterations

PDGF-BB, a robust pleiotropic factor, is neuroprotective in HIV protein gp120- and Tat-mediated apoptosis (Cheng and Mattson, 1995; Peng et al., 2008; Zhu et al., 2009) and has also been shown to restore neuronal differentiation in neural progenitor cells in presence of both HIV Tat and cocaine (Yang et al., 2015). We (Peng et al., 2010) have previously demonstrated that PDGF-BB induces expression of synaptic plasticity gene Arc/Arg3.1 in hippocampal neurons, suggesting that it may be a key player in the regulation of synaptic plasticity, although the underlying mechanisms remain unclear.

Our data indicate that treatment of morphine-exposed neurons with PDGF-BB ameliorated morphine-mediated synaptic alterations in hippocampal neurons. This effect of PDGF-BB was at the level of inhibition of ROS production after MOR activation, leading, in turn, to inhibition of downstream ER stress and autophagy pathways, ultimately leading to preservation of excitatory and inhibitory synapses.

Thus, our results strongly support a model in which morphine exposure leads to sequential generation of ROS, initiation of ER stress, and enhanced autophagic activities to modulate both excitatory and inhibitory synaptic densities in the hippocampal neurons. Furthermore, we provide a novel neuroprotective role of PDGF-BB in blocking morphine-mediated synaptic alterations. It can thus be envisioned that therapeutic strategies aimed at activating PDGF-BB signaling could be beneficial in reversing morphine-mediated cognitive decline.

Materials and methods

Reagents

Morphine (M8777-250MG; Sigma-Aldrich), naltrexone (N3136-100MG; Sigma-Aldrich), PDGF-BB (220-BB-050; R&D Systems), PBN (B7263-1G; Sigma-Aldrich), apocynin (sc-203321; Santa Cruz Biotechnology, Inc.), mitoTEMPO (SML0737; Sigma-Aldrich), 4-PBA (50–230-7444; Thermo Fisher Scientific), salubrinal (SML0951; Sigma-Aldrich), wortmannin (W3144; Sigma-Aldrich), 3-MA (M9281; Sigma-Aldrich), and bafilomycin (B1793; Sigma-Aldrich) were obtained from commercial vendors as described.

DNA constructs

The pCAGGs-IRES-eGFP plasmid has been previously described and validated (Arikkath et al., 2008). pCMV-GFP-LC3 expression vector was provided by H. Fox (University of Nebraska Medical Center, Omaha, NE; Alirezaei et al., 2008). Both PGK-GFP-shATG7 and PGK-GFP-scramble were gifts from A.M. Cuervo (Albert Einstein College of Medicine, Bronx, NY; Rodríguez-Muela et al., 2013).

Animals

All animal procedures were performed according to the protocols approved by the Institutional Animal Care and Use Committee of the University of Nebraska Medical Center and the National Institutes of Health. Sprague-Dawley rats and C57BL/6N mice were purchased from Charles River. All animals were housed under constant temperature and humidity on a 12-h light/dark cycle with available access to food and water ad libitum. 2-mo-old male C57BL/6N mice were equally divided in two groups: saline and morphine. Morphine sulfate was dissolved in 0.9% sodium chloride (NDC 0409–4888-12; Hospira). The morphine-treated group was administrated intraperitoneal injections of morphine, three times a day every 8 h, at an initial dose of 10 mg/kg with an increment of 5 mg/kg every day for 6 d. Saline groups received a comparable volume of saline (as morphine group) daily. All mice were sacrificed 1 h after the last morphine/saline injection on the last day.

Primary neuron cultures

All experimental procedures were approved by the University of Nebraska Medical Center Institutional Animal Care and Use Committee. Primary rat hippocampal neurons were obtained from E18 rat hippocampi as previously described (Arikkath et al., 2009; Beaudoin et al., 2012). In brief, after dissociation of the dissected brain hippocampi in HBSS (14170112; Invitrogen) supplemented with 0.25% trypsin (LS003707; Worthington Biochemical Corporation), primary neurons were plated at a density of 7.5×10^4 on poly-L-lysine–coated 18-mm glass coverslips. Cultures were maintained in Neurobasal medium (21103049; Invitrogen) with B27 supplement (17504044; Invitrogen), Glutamax (3505061; Invitrogen), and penicillin-streptomycin (15070063; Invitrogen) at 37°C with 5% CO_2. Cytosine β-D-arabinofuranoside (1 µM; C1768; Sigma-Aldrich) was added on DIV 2, and all media were replaced on DIV 3. Half of the media was replaced twice every week. Transfection was performed on DIV 7 using Lipofectamine 2000 (11668027; Invitrogen) as indicated by the manufacturer. Half of the media was replaced 12 h after transfection. Neurons (DIV 20) were treated with morphine (10 µM) for 24 h after 1-h pretreatment of pharmacological inhibitors. Primary hippocampal neurons were treated with PDGF-BB (20 ng/ml) for 24 h immediately after morphine exposure.

Immunocytochemistry

For immunocytochemistry, primary rat hippocampal neurons were plated on coverslips treated with the respective agents for 24–48 h, followed by fixing with 4% PFA and 4% sucrose in PBS for 20 min at room temperature and permeabilization with 0.1% Triton X-100 (BP151-1; Thermo Fisher Scientific). Neurons were then incubated in 5% normal goat serum PBS buffer for 1 h at room temperature followed by addition of respective antibodies: PSD95 (1:500; catalog no. ab18258, lot no. RRID:AB_444362; Abcam), gephyrin (1:1,000; catalog number 147 011, lot number RRID:AB_88771; Synaptic Systems), ATG7 (1:100; catalog no. R-161-100, lot no. RRID:AB_2492996; Biosensis) or vGlut1 (1:4,000; catalog no. AB5905, lot no. RRID:AB_23017501; EMD Millipore), and GAD65 (1:100; catalog no. GAD-6, lot no. RRID:AB_528264; Developmental Studies Hybridoma Bank) overnight at 4°C. This was followed by addition of the secondary Alexa Fluor 555 goat anti–rabbit (1:500; catalog no. A27039, lot no. RRID:AB_2536100; Thermo Fisher Scientific), Alexa Fluor 555 goat anti–mouse (1:500; catalog no. A-21424, lot no. RRID:AB_2535845; Thermo Fisher Scientific) or Alexa Fluor 488 goat anti–guinea pig

(1:500; catalog no. A-11073, lot no. RRID:AB_2534117; Thermo Fisher Scientific), and Alexa Fluor 555 goat anti-rabbit (1:500; catalog no. A27039, lot no. RRID:AB_2536100; Thermo Fisher Scientific), respectively. Cells were mounted with Prolong Gold antifade reagent with DAPI (P36935; Thermo Fisher Scientific).

Immunohistochemistry

Under anesthesia, animals were perfused with chilled 4% PFA. Sections encompassing the entire hippocampus were sectioned at 12 µm on a cryostat and incubated with a blocking buffer containing 5% normal goat serum and 0.2% Triton X-100 (Thermo Fisher Scientific) for 1 h at room temperature followed by addition of respective antibody pairs: vGlut1 (1:4,000; catalog no. AB5905, lot no. RRID:AB_2301751; EMD Millipore) and GAD65 (1:100; catalog no. GAD-6, lot no. RRID:AB_528264; Developmental Studies Hybridoma Bank) and PSD95 (1:500; catalog no. ab18258, lot no. RRID:AB_444362; Abcam) and gephyrin (1:1,000; catalog no. 147 011, lot no. RRID:AB_88771; Synaptic Systems) and incubated overnight at 4°C. The next day, the sections were washed followed by incubation with Alexa Fluor 488 goat anti–guinea pig (1:500; catalog no. A-11073, lot no. RRID:AB_2534117; Thermo Fisher Scientific) and Alexa Fluor 555 goat anti–rabbit (1:500; catalog no. A27039, lot no. RRID:AB_2536100; Thermo Fisher Scientific) or Alexa Fluor 488 goat anti–rabbit (1:500; catalog no. A11008, lot no. RRID:AB_10563748; Thermo Fisher Scientific) and Alexa Fluor 555 goat anti–mouse (1:500; catalog no. A-21424, lot no. RRID:AB_2535845; Thermo Fisher Scientific), respectively, in 0.5% BSA and 0.2% Triton X-100 at room temperature for 2 h, followed by mounting with Prolong Gold antifade reagent (P36935; Thermo Fisher Scientific). Every eighth section from each mouse was used to quantify synapses using presynaptic or postsynaptic markers in the hippocampus.

Microscopy acquisition and spine architecture quantitation

Imaging was performed on an inverted LSM 700 microscope with a 40× objective and a digital zoom of 4× (ZEISS). Contrast and brightness of overall images were consistent in each set of experiments. For primary neurons in vitro, the number of synapses and dendritic spines were counted manually in Zen 2010 SP1 (ZEISS) using a digital zoom of 4× with Z-stack projection. These measurements were obtained on one dendrite per neuron within 80 µm from the cell body. Data were obtained from four independent cultures. The numbers of synapses and dendritic spines are indicated on the bar graph. For in vivo, the number of synapses in the striatum lucidum and radiatum of hippocampus were measured using Bitplane Imaris 7.6.5 software (RRID:SCR_007370; Imaris).

Electrophysiology

Whole-cell recordings were performed on primary hippocampal neurons (DIV 19–21) seeded on coverslips. Recording electrodes (tip resistance 5.0–8.0 MΩ) were pulled from borosilicate glass micropipettes (World Precision Instruments) with a P-97 micropipette puller (Sutter Instruments Company). The intracellular solution contained: 120 mM potassium-gluconate, 10 mM KCl, 5 mM NaCl, 1 mM $CaCl_2$, 2 mM $MgCl_2$, 11 mM EGTA, 10 mM Hepes, 2 mM Mg-ATP, and 1 mM GTP, adjusted pH to 7.3 with KOH. The extracellular solution contained: 140 mM NaCl, 5 mM KCl, 2.5 mM $CaCl_2$, 10 mM Hepes, and 10 mM glucose, adjusted pH to 7.4 with NaOH, and extracellular solution was preoxygenated for 30 min in before recording. Picrotoxin (150 µM) was added to bath solutions to block GABA-A receptor–mediated currents, which allowed the recording of mEPSCs. The α-amino-3-hydroxy-5-methyl-4-isoxazolepropionic acid (AMPA) and kainate receptor blocker 6,7-dinitroquinoxaline-2,3-dione (10 µM) and the voltage-gated sodium channel blocker tetrodotoxin (1 µM) were added in the bath solutions for the measurement of miniature IPSCs (mIPSCs). The recording electrodes were positioned by a Burleigh micromanipulator (PC-5000; EXFO). The cells were allowed to stabilize for 3–5 min after establishment of the whole-cell patch configuration. Cell capacitance was compensated >70%. The mEPSCs and mIPSCs were recorded at holding potential at −60 mV during voltage clamping. Current signals were filtered at 1 kHz and digitized at 5 kHz using Digidata 1440A digitizer (Molecular Devices). The current traces were displayed and recorded in a computer using Clampex 8.2 (Molecular Devices). All experiments were done at room temperature (22 to 23°C). Frequencies of mEPSCs and mIPSCs were analyzed by Clampfit 8.2 (Molecular Devices) and graphed using Origin 8.5 (OriginLab).

Western blotting

Treated cells were lysed using the Mammalian Cell Lysis kit (MCL1-1KT; Sigma-Aldrich). Equal amounts of proteins were electrophoresed in a SDS-PAGE (10%) under reducing conditions followed by transfer to polyvinylidene fluoride membranes. The blots were blocked with 5% BSA in PBS. The Western blots were then probed with respective antibodies recognizing the vGlut1 (1:5,000; catalog no. AB5905, lot no. RRID:AB_2301751; EMD Millipore), PSD95 (1:1,000; catalog no. ab18258; lot no. RRID:AB_444362; Abcam), GAD65 (1:1,000; catalog no. NBP1-33284, lot no. RRID:AB_10004060; Novus Biologicals), gephyrin (1:250; catalog no. 610584, lot no. RRID:AB_397929; BD), BIP (1:1,000; catalog no. 610978, lot no. RRID:AB_398291; BD), pPERK (1:250; catalog no. sc-32577, lot no. RRID:AB_2293243; Santa Cruz Biotechnology, Inc.), PERK (1:250; catalog no. sc-13073, lot no. RRID:AB_2230863; Santa Cruz Biotechnology, Inc.), IRE1α (1:500; catalog no. sc-20790, lot no. RRID:AB_2098712; Santa Cruz Biotechnology, Inc.), ATF6 (1:1,000; catalog no. ab37149, lot no. RRID:AB_725571; Abcam), Beclin1 (1:1,000; catalog no. sc-11427, lot no. RRID:AB_2064465; Santa Cruz Biotechnology, Inc.), ATG5 (1:1,000; catalog no. NB110-53818, lot no. RRID:AB_828587, Novus Biologicals), p62 (1:1,000; catalog no. 50–507-55, lot no. RRID: AB_2571590; Thermo Fisher Scientific), LC3 (1:2,000; catalog no. NB100-2220, lot no. RRID:AB_10003146; Novus Biologicals), and β-actin (1:5,000; catalog no. A1978, lot no. RRID:AB_476692; Sigma-Aldrich). The secondary antibodies were horseradish peroxidase–conjugated to goat anti–mouse/rabbit/guinea pig IgG (1:5,000; catalog no. sc-2005, lot no. RRID:AB_631736, Santa Cruz Biotechnology, Inc.; catalog no. sc-2004, lot no. RRID:AB_631746, Santa Cruz Biotechnology, Inc.; and catalog no. 61-4620, lot no. RRID:AB_2533926, Thermo Fisher Scientific) as described previously (Yang et al., 2016).

Assessment of cellular ROS production: H_2DCFDA assays

H_2DCFDA (D339; Thermo Fisher Scientific) was used to measure total cellular ROS levels in hippocampal neurons according to the manufacturer's recommended protocol. Neurons were seeded on either 96-well plates for fluorescence readout or coverslips in 12-well plates for imaging. After neurons were treated according to the experimental conditions, medium was removed, and cells were incubated with 25 µM H_2DCFDA working solution for 30 min at 37°C. Hoechst 33342 (1.0 µM; H3570; Hoechst; Thermo Fisher Scientific) was added to H_2DCFDA working solution during the last 5 min. Cells were subsequently rinsed in PBS, and the change in H_2DCFDA fluorescence in 96-well plates was detected in a spectrofluorimeter set at 485-nm excitation and 530-nm emission, whereas Hoechst 33342 (Thermo Fisher Scientific) was measured at 350-nm excitation and 461-nm emission. The level of intracellular ROS was indicated by the readouts of H_2DCFDA and standardized according to the Hoechst 33342

(Thermo Fisher Scientific) levels. Neurons were mounted on coverslips and observed under an inverted LSM 700 confocal microscope using a 40× objective (ZEISS).

Statistical analysis

All data are presented as mean ± SD and were analyzed using the Student's *t* test or analysis of variance (ANOVA) model with post hoc test to compare means between each group. All data were graphed, and statistical analyses were performed using Prism 6 (GraphPad Software). Results were considered statistically significant if probability levels were <0.05.

Online supplemental material

Fig. S1 shows that morphine alters the densities of excitatory and inhibitory synapses in the hippocampus. Fig. S2 shows morphine-mediated alterations of synaptic proteins in the brain. Fig. S3 shows morphine-mediated transcriptional alterations of synaptic proteins in the brain. Fig. S4 illustrates that PGK-GFP-shATG7 plasmids successfully knock down ATG7 expression level in primary hippocampal neurons.

Acknowledgments

We are grateful to Dr. Ana Maria Cuervo for the PGK-GFP-shATG7 and PGK-GFP-scramble constructs and to Dr. Howard Fox for the pCMV-GFP-LC3 construct.

This work is supported by National Institutes of Health grants DA033150, DA033614, DA035203, DA036157 (to S. Buch), and P30GM110768, and Alzheimer's Association and Munroe-Meyer Institute Startup funds (to J. Arikkath). L. Yuan is supported by a University of Nebraska Medical Center graduate fellowship.

The authors declare no competing financial interests.

Submitted: 17 May 2016
Accepted: 26 September 2016

References

Alirezaei, M., W.B. Kiosses, C.T. Flynn, N.R. Brady, and H.S. Fox. 2008. Disruption of neuronal autophagy by infected microglia results in neurodegeneration. *PLoS One.* 3:e2906. http://dx.doi.org/10.1371/journal.pone.0002906

Arikkath, J., I. Israely, Y. Tao, L. Mei, X. Liu, and L.F. Reichardt. 2008. Erbin controls dendritic morphogenesis by regulating localization of delta-catenin. *J. Neurosci.* 28:7047–7056. http://dx.doi.org/10.1523/JNEUROSCI.0451-08.2008

Arikkath, J., I.F. Peng, Y.G. Ng, I. Israely, X. Liu, E.M. Ullian, and L.F. Reichardt. 2009. Delta-catenin regulates spine and synapse morphogenesis and function in hippocampal neurons during development. *J. Neurosci.* 29:5435–5442. http://dx.doi.org/10.1523/JNEUROSCI.0835-09.2009

Beaudoin, G.M. III, S.H. Lee, D. Singh, Y. Yuan, Y.G. Ng, L.F. Reichardt, and J. Arikkath. 2012. Culturing pyramidal neurons from the early postnatal mouse hippocampus and cortex. *Nat. Protoc.* 7:1741–1754. http://dx.doi.org/10.1038/nprot.2012.099

Bhat, R.S., M. Bhaskaran, A. Mongia, N. Hitosugi, and P.C. Singhal. 2004. Morphine-induced macrophage apoptosis: oxidative stress and strategies for modulation. *J. Leukoc. Biol.* 75:1131–1138. http://dx.doi.org/10.1189/jlb.1203639

Brennan, A.M., S.W. Suh, S.J. Won, P. Narasimhan, T.M. Kauppinen, H. Lee, Y. Edling, P.H. Chan, and R.A. Swanson. 2009. NADPH oxidase is the primary source of superoxide induced by NMDA receptor activation. *Nat. Neurosci.* 12:857–863. http://dx.doi.org/10.1038/nn.2334

Cai, Y., J. Arikkath, L. Yang, M.L. Guo, P. Periyasamy, and S. Buch. 2016a. Interplay of endoplasmic reticulum stress and autophagy in neurodegenerative disorders. *Autophagy.* 12:225–244. http://dx.doi.org/10.1080/15548627.2015.1121360

Cai, Y., H. Kong, Y.B. Pan, L. Jiang, X.X. Pan, L. Hu, Y.N. Qian, C.Y. Jiang, and W.T. Liu. 2016b. Procyanidins alleviates morphine tolerance by inhibiting activation of NLRP3 inflammasome in microglia. *J. Neuroinflammation.* 13:53. http://dx.doi.org/10.1186/s12974-016-0520-z

Cao, V.Y., Y. Ye, S. Mastwal, M. Ren, M. Coon, Q. Liu, R.M. Costa, and K.H. Wang. 2015. Motor learning consolidates Arc-expressing neuronal ensembles in secondary motor cortex. *Neuron.* 86:1385–1392. http://dx.doi.org/10.1016/j.neuron.2015.05.022

Cheng, B., and M.P. Mattson. 1995. PDGFs protect hippocampal neurons against energy deprivation and oxidative injury: evidence for induction of antioxidant pathways. *J. Neurosci.* 15:7095–7104.

Fields, H.L. 2011. The doctor's dilemma: opiate analgesics and chronic pain. *Neuron.* 69:591–594. http://dx.doi.org/10.1016/j.neuron.2011.02.001

Fields, H.L., and E.B. Margolis. 2015. Understanding opioid reward. *Trends Neurosci.* 38:217–225. http://dx.doi.org/10.1016/j.tins.2015.01.002

Froemke, R.C., M.M. Merzenich, and C.E. Schreiner. 2007. A synaptic memory trace for cortical receptive field plasticity. *Nature.* 450:425–429. http://dx.doi.org/10.1038/nature06289

Gomes, A., E. Fernandes, and J.L. Lima. 2005. Fluorescence probes used for detection of reactive oxygen species. *J. Biochem. Biophys. Methods.* 65:45–80. http://dx.doi.org/10.1016/j.jbbm.2005.10.003

Gouty-Colomer, L.A., B. Hosseini, I.M. Marcelo, J. Schreiber, D.E. Slump, S. Yamaguchi, A.R. Houweling, D. Jaarsma, Y. Elgersma, and S.A. Kushner. 2016. Arc expression identifies the lateral amygdala fear memory trace. *Mol. Psychiatry.* 21:364–375. http://dx.doi.org/10.1038/mp.2015.18

Guo, M.L., K. Liao, P. Periyasamy, L. Yang, Y. Cai, S.E. Callen, and S. Buch. 2015. Cocaine-mediated microglial activation involves the ER stress-autophagy axis. *Autophagy.* 11:995–1009. http://dx.doi.org/10.1080/15548627.2015.1052205

Hearing, M.C., J. Jedynak, S.R. Ebner, A. Ingebretson, A.J. Asp, R.A. Fischer, C. Schmidt, E.B. Larson, and M.J. Thomas. 2016. Reversal of morphine-induced cell-type-specific synaptic plasticity in the nucleus accumbens shell blocks reinstatement. *Proc. Natl. Acad. Sci. USA.* 113:757–762. http://dx.doi.org/10.1073/pnas.1519248113

Hetz, C., and B. Mollereau. 2014. Disturbance of endoplasmic reticulum proteostasis in neurodegenerative diseases. *Nat. Rev. Neurosci.* 15:233–249. http://dx.doi.org/10.1038/nrn3689

Hill, J.L., and J.P. Zacny. 2000. Comparing the subjective, psychomotor, and physiological effects of intravenous hydromorphone and morphine in healthy volunteers. *Psychopharmacology (Berl.).* 152:31–39. http://dx.doi.org/10.1007/s002130000500

Horvath, R.J., E.A. Romero-Sandoval, and J.A. De Leo. 2010. Inhibition of microglial P2X4 receptors attenuates morphine tolerance, Iba1, GFAP and mu opioid receptor protein expression while enhancing perivascular microglial ED2. *Pain.* 150:401–413. http://dx.doi.org/10.1016/j.pain.2010.02.042

Huang, R.R., W. Hu, Y.Y. Yin, Y.C. Wang, W.P. Li, and W.Z. Li. 2015. Chronic restraint stress promotes learning and memory impairment due to enhanced neuronal endoplasmic reticulum stress in the frontal cortex and hippocampus in male mice. *Int. J. Mol. Med.* 35:553–559. http://dx.doi.org/10.3892/ijmm.2014.2026

Hyman, S.E., R.C. Malenka, and E.J. Nestler. 2006. Neural mechanisms of addiction: The role of reward-related learning and memory. *Annu. Rev. Neurosci.* 29:565–598. http://dx.doi.org/10.1146/annurev.neuro.29.051605.113009

Ibi, M., K. Matsuno, M. Matsumoto, M. Sasaki, T. Nakagawa, M. Katsuyama, K. Iwata, J. Zhang, S. Kaneko, and C. Yabe-Nishimura. 2011. Involvement of NOX1/NADPH oxidase in morphine-induced analgesia and tolerance. *J. Neurosci.* 31:18094–18103. http://dx.doi.org/10.1523/JNEUROSCI.4136-11.2011

Keller, A., A. Westenberger, M.J. Sobrido, M. García-Murias, A. Domingo, R.L. Sears, R.R. Lemos, A. Ordoñez-Ugalde, G. Nicolas, J.E. da Cunha, et al. 2013. Mutations in the gene encoding PDGF-B cause brain calcifications in humans and mice. *Nat. Genet.* 45:1077–1082. http://dx.doi.org/10.1038/ng.2723

Koob, G.F., and N.D. Volkow. 2010. Neurocircuitry of addiction. *Neuropsychopharmacology.* 35:217–238. http://dx.doi.org/10.1038/npp.2009.110

Kurita, G.P., P. Sjøgren, O. Ekholm, S. Kaasa, J.H. Loge, I. Poviloniene, and P. Klepstad. 2011. Prevalence and predictors of cognitive dysfunction in opioid-treated patients with cancer: A multinational study. *J. Clin. Oncol.* 29:1297–1303. http://dx.doi.org/10.1200/JCO.2010.32.6884

Le Merrer, J., J.A. Becker, K. Befort, and B.L. Kieffer. 2009. Reward processing by the opioid system in the brain. *Physiol. Rev.* 89:1379–1412. http://dx.doi.org/10.1152/physrev.00005.2009

Marder, E., and J.M. Goaillard. 2006. Variability, compensation and homeostasis in neuron and network function. *Nat. Rev. Neurosci.* 7:563–574. http://dx.doi.org/10.1038/nrn1949

Martínez, G., R.L. Vidal, P. Mardones, F.G. Serrano, A.O. Ardiles, C. Wirth, P. Valdés, P. Thielen, B.L. Schneider, B. Kerr, et al. 2016. Regulation of memory formation by the transcription factor XBP1. *Cell Reports.* 14:1382–1394. http://dx.doi.org/10.1016/j.celrep.2016.01.028

Martini-Stoica, H., Y. Xu, A. Ballabio, and H. Zheng. 2016. The autophagy-lysosomal pathway in neurodegeneration: A TFEB perspective. *Trends Neurosci.* 39:221–234. http://dx.doi.org/10.1016/j.tins.2016.02.002

Massaad, C.A., and E. Klann. 2011. Reactive oxygen species in the regulation of synaptic plasticity and memory. *Antioxid. Redox Signal.* 14:2013–2054. http://dx.doi.org/10.1089/ars.2010.3208

Mazei-Robison, M.S., J.W. Koo, A.K. Friedman, C.S. Lansink, A.J. Robison, M. Vinish, V. Krishnan, S. Kim, M.A. Siuta, A. Galli, et al. 2011. Role for mTOR signaling and neuronal activity in morphine-induced adaptations in ventral tegmental area dopamine neurons. *Neuron.* 72:977–990. http://dx.doi.org/10.1016/j.neuron.2011.10.012

Menzies, F.M., A. Fleming, and D.C. Rubinsztein. 2015. Compromised autophagy and neurodegenerative diseases. *Nat. Rev. Neurosci.* 16:345–357. http://dx.doi.org/10.1038/nrn3961

Nelson, S.B., and V. Valakh. 2015. Excitatory/inhibitory balance and circuit homeostasis in autism spectrum disorders. *Neuron.* 87:684–698. http://dx.doi.org/10.1016/j.neuron.2015.07.033

Pal, A., and S. Das. 2013. Chronic morphine exposure and its abstinence alters dendritic spine morphology and upregulates Shank1. *Neurochem. Int.* 62:956–964. http://dx.doi.org/10.1016/j.neuint.2013.03.011

Peng, F., N. Dhillon, S. Callen, H. Yao, S. Bokhari, X. Zhu, H.H. Baydoun, and S. Buch. 2008. Platelet-derived growth factor protects neurons against gp120-mediated toxicity. *J. Neurovirol.* 14:62–72. http://dx.doi.org/10.1080/13550280701809084

Peng, F., H. Yao, X. Bai, X. Zhu, B.C. Reiner, M. Beazely, K. Funa, H. Xiong, and S. Buch. 2010. Platelet-derived growth factor-mediated induction of the synaptic plasticity gene Arc/Arg3.1. *J. Biol. Chem.* 285:21615–21624. http://dx.doi.org/10.1074/jbc.M110.107003

Robinson, T.E., G. Gorny, V.R. Savage, and B. Kolb. 2002. Widespread but regionally specific effects of experimenter- versus self-administered morphine on dendritic spines in the nucleus accumbens, hippocampus, and neocortex of adult rats. *Synapse.* 46:271–279. http://dx.doi.org/10.1002/syn.10146

Rodríguez-Muela, N., H. Koga, L. García-Ledo, P. de la Villa, E.J. de la Rosa, A.M. Cuervo, and P. Boya. 2013. Balance between autophagic pathways preserves retinal homeostasis. *Aging Cell.* 12:478–488. http://dx.doi.org/10.1111/acel.12072

Sandi, C., and J. Haller. 2015. Stress and the social brain: Behavioural effects and neurobiological mechanisms. *Nat. Rev. Neurosci.* 16:290–304. http://dx.doi.org/10.1038/nrn3918

Shadel, G.S., and T.L. Horvath. 2015. Mitochondrial ROS signaling in organismal homeostasis. *Cell.* 163:560–569. http://dx.doi.org/10.1016/j.cell.2015.10.001

Shehata, M., H. Matsumura, R. Okubo-Suzuki, N. Ohkawa, and K. Inokuchi. 2012. Neuronal stimulation induces autophagy in hippocampal neurons that is involved in AMPA receptor degradation after chemical long-term depression. *J. Neurosci.* 32:10413–10422. http://dx.doi.org/10.1523/JNEUROSCI.4533-11.2012

Smolen, P., Y. Zhang, and J.H. Byrne. 2016. The right time to learn: Mechanisms and optimization of spaced learning. *Nat. Rev. Neurosci.* 17:77–88. http://dx.doi.org/10.1038/nrn.2015.18

Tang, G., K. Gudsnuk, S.H. Kuo, M.L. Cotrina, G. Rosoklija, A. Sosunov, M.S. Sonders, E. Kanter, C. Castagna, A. Yamamoto, et al. 2014. Loss of mTOR-dependent macroautophagy causes autistic-like synaptic pruning deficits. *Neuron.* 83:1131–1143. http://dx.doi.org/10.1016/j.neuron.2014.07.040

Tang, Z., P. Arjunan, C. Lee, Y. Li, A. Kumar, X. Hou, B. Wang, P. Wardega, F. Zhang, L. Dong, et al. 2010. Survival effect of PDGF-CC rescues neurons from apoptosis in both brain and retina by regulating GSK3beta phosphorylation. *J. Exp. Med.* 207:867–880. http://dx.doi.org/10.1084/jem.20091704

Uehara, T., T. Nakamura, D. Yao, Z.Q. Shi, Z. Gu, Y. Ma, E. Masliah, Y. Nomura, and S.A. Lipton. 2006. S-nitrosylated protein-disulphide isomerase links protein misfolding to neurodegeneration. *Nature.* 441:513–517. http://dx.doi.org/10.1038/nature04782

Vacca, V., S. Marinelli, S. Luvisetto, and F. Pavone. 2013. Botulinum toxin A increases analgesic effects of morphine, counters development of morphine tolerance and modulates glia activation and μ opioid receptor expression in neuropathic mice. *Brain Behav. Immun.* 32:40–50. http://dx.doi.org/10.1016/j.bbi.2013.01.088

Wang, L., Y. Yu, D.C. Chow, F. Yan, C.C. Hsu, F. Stossi, M.A. Mancini, T. Palzkill, L. Liao, S. Zhou, et al. 2015. Characterization of a steroid receptor coactivator small molecule stimulator that overstimulates cancer cells and leads to cell stress and death. *Cancer Cell.* 28:240–252. http://dx.doi.org/10.1016/j.ccell.2015.07.005

Yang, L., X. Chen, G. Hu, Y. Cai, K. Liao, and S. Buch. 2015. Mechanisms of platelet-derived growth factor-BB in restoring HIV Tat-cocaine-mediated impairment of neuronal differentiation. *Mol. Neurobiol.* http://dx.doi.org/10.1007/s12035-015-9536-0.

Yang, L., H. Yao, X. Chen, Y. Cai, S. Callen, and S. Buch. 2016. Role of sigma receptor in cocaine-mediated induction of glial fibrillary acidic protein: Implications for HAND. *Mol. Neurobiol.* 53:1329–1342. http://dx.doi.org/10.1007/s12035-015-9094-5

Younce, C.W., and P.E. Kolattukudy. 2010. MCP-1 causes cardiomyoblast death via autophagy resulting from ER stress caused by oxidative stress generated by inducing a novel zinc-finger protein, MCPIP. *Biochem. J.* 426:43–53. http://dx.doi.org/10.1042/BJ20090976

Zhang, H., and E.H. Baehrecke. 2015. Eaten alive: Novel insights into autophagy from multicellular model systems. *Trends Cell Biol.* 25:376–387. http://dx.doi.org/10.1016/j.tcb.2015.03.001

Zhao, L., Y. Zhu, D. Wang, M. Chen, P. Gao, W. Xiao, G. Rao, X. Wang, H. Jin, L. Xu, et al. 2010. Morphine induces Beclin 1- and ATG5-dependent autophagy in human neuroblastoma SH-SY5Y cells and in the rat hippocampus. *Autophagy.* 6:386–394. http://dx.doi.org/10.4161/auto.6.3.11289

Zheng, H., Y. Zeng, J. Chu, A.Y. Kam, H.H. Loh, and P.Y. Law. 2010. Modulations of NeuroD activity contribute to the differential effects of morphine and fentanyl on dendritic spine stability. *J. Neurosci.* 30:8102–8110. http://dx.doi.org/10.1523/JNEUROSCI.6069-09.2010

Zhu, X., H. Yao, F. Peng, S. Callen, and S. Buch. 2009. PDGF-mediated protection of SH-SY5Y cells against Tat toxin involves regulation of extracellular glutamate and intracellular calcium. *Toxicol. Appl. Pharmacol.* 240:286–291. http://dx.doi.org/10.1016/j.taap.2009.06.020